Cellular Physiology and Biochemistry

Cell Physiol Biochem 2014;33:1921-1932
DOI: 10.1159/000362969
Published online: June 27, 2014
Accepted:

Karger Open access

1421-9778/14/0336-1921$39.50/0

Original Paper

Neuronostatin Attenuates Myocardial Contractile Function through Inhibition of Sarcoplasmic Reticulum Ca^{2+}-ATPase in Murine Heart

Xiaoling Zhu[a,c,e] Nan Hu[c,e] Xiyao Chen[b,e] Miao-Zhang Zhu[b] Hailong Dong[a] Xihui Xu[c] Fuling Luo[c] Yinan Hua[c] Sreejayan Nair[c] Willis K. Samson[d] Lize Xiong[a] Jun Ren[c]

[a]Department of Anesthesiology, Xijing Hospital, [b]Department of Physiology, the Fourth Military Medical University, Xi'an, China; [c]Center for Cardiovascular Research and Alternative Medicine, University of Wyoming College of Health Sciences, Laramie, WY, USA; [d]Department of Pharmacological and Physiological Science, St. Louis University School of Medicine, St. Louis, MO, USA

Key Words
Neuronostatin • Cardiac • Contractile • SERCA • AMPK

Abstract
Background/Aims: Neuronostatin, derived from the somatostatin preprohormone, was recently identified to be produced by several tissues exerting a role in cardiovascular regulation and metabolism. Nonetheless, the precise mechanism behind neuronostatin-elicited myocardial responses remains elusive. ***Methods:*** This study was designed to elucidate the impact of neuronostatin on cardiac contractile function and the underlying mechanism of action involved. Adult male C57 BL/6 mice were subjected to a bolus injection of neuronostatin (50 μg/kg, i.p.). Echocardiographic, cardiomyocyte contractile and intracellular Ca^{2+} handling properties were monitored to evaluate the effect of neuronostatin on cardiac function. Western blot analysis was used to examine potential signaling mechanisms involved. ***Results:*** Neuronostatin administration suppressed myocardial and cardiomyocyte contractile function and disturbed intracellular Ca^{2+} homeostasis. We observed enlarged LVESD (with unchanged LVEDD), reduced fractional shortening, depressed peak shortening, maximal velocity of shortening/relengthening, resting and electrically-stimulated rise in intracellular Ca^{2+}, and prolonged relengthening duration in hearts from neuronostatin-treated mice. These effects were accompanied by downregulation of phosphorylation of sarcoplasmic reticulum Ca^{2+}-ATPase (SERCA) and phospholamban (PLB) and activation of AMPK. ***Conclusion:*** Our data suggest that the cardiac depressant properties of neuronostatin possibly associated with loss of SERCA phosphorylation and AMPK activation. These findings revealed a potent inhibitory capacity for neuronostatin on cardiac function, the physiological relevance of which deserves further study.

X. Zhu, N. Hu and X. Chen contributed equally

Dr. Lize Xiong,
and Dr. Jun Ren

Department of Anesthesiology, Xijing Hospital, Fourth Military Medical University, Xi'an, Shaanxi Province (China)
and University of Wyoming College of Health Sciences, Laramie, WY 82071 (USA)
E-Mail mzkxlz@126.com and E-Mail jren@uwyo.edu

Introduction

Somatostatin, a cyclic peptide originally identified as an inhibitor for growth hormone and thyroid-stimulating hormone secretions, plays an important role in gastrointestinal endocrinology [1] and cardiovascular regulation [2]. Somatostatin-like immunoreactivity has been identified in hearts from a number of mammalian species including human [3]. Not surprisingly, somatostatin displays pronounced cardiotropic properties. Somatostatin analogs exert a variety of myocardial morphological, functional and hemodynamic effects in patients with acromegaly [4]. Nonetheless, controversy remains with regards to the cardiac contractile impact of somatostatin analogs. Osadchii and colleagues reported that somatostatin depresses myocardial contractility, diminishes cardiac output and decreases heart rate [3]. In addition, somatostatin suppresses atrial contractile function in isolated guinea-pig hearts [5]. The precise mechanisms underlying the cardiac effects of somatostatin remain elusive.

A novel peptide encoded by the somatostatin gene was recently identified and named neuronostatin [6]. Neuronostatin, a 13-amino acid peptide (Leu-Arg-Gln-Phe-Leu- Gln-Lys-Ser-Leu-Ala-Ala-Ala-Ala-NH2) reminiscent of somatostatin, is found in central and peripheral organs to play a role in the regulation of hormonal and cardiac function [6, 7]. Neuronostatin has been reported to possess significant roles in a wide variety of biological actions including food intake, drinking behavior and blood pressure. More recent evidence from our group suggested that neuronostatin inhibits cardiac contractile function via a protein kinase A (PKA)- and c-Jun N-terminal kinase (JNK)-dependent mechanism [8]. In addition, neuronostatin attenuates endothelin-1 (ET-1)-induced left ventricular contractility in isolated rat hearts via p38 MAPK and JNK phosphorylation-dependent mechanisms [9].

Tight control of cytosolic Ca^{2+} removal is crucial for the maintenance of normal, cardiac function. Sarcoplasmic reticulum Ca^{2+}- ATPase (SERCA2a) and its regulator phospholamban (PLB), play an essential role in intracellular Ca^{2+} homeostasis and cycling in heart [10, 11]. To this end, the present study was designed to examine the echocardiographic and cardiomyocyte contractile responses of neuronostatin *in vivo*. To explore the potential role of intracellular Ca^{2+} handling in neuronostatin-elicited myocardial contractile response, if any, intracellular Ca^{2+} property was evaluated including the main intracellular Ca^{2+} regulatory proteins [SERCA2a, PLB, Ca^{2+}/calmodulin-dependent protein kinase II (CaMK II) and troponin I]. We further monitored several key signal pathways such as Akt, AMP-dependent kinase (AMPK), extracellular signal-regulated kinase 1/2 (ERK1/2), p38 MAPK and JNK, which are reported to mediate neuronostatin-mediated physiological actions [12].

Materials and Methods

Experimental animal and neuronostatin treatment

The experimental procedures carried out in this study were approved by the University of Wyoming Institutional Animal Use and Care Committee (Laramie, WY, USA) and were in compliance with the Guide for the Care and Use of Laboratory Animals published by the US National Institutes of Health (NIH Publication No. 85-23, revised 1996). In brief, 3-month-old adult male C57BL/6 mice were housed in a temperature-controlled environment (22.8 ± 2.0°C, 45–50% humidity) with a 12:12h light/dark cycle with free access to food and tap water. For neuronostatin challenge *in vivo*, 3-month-old adult C57BL/6 male mice were randomly divided into two groups and to receive neuronostatin (50 μg/kg, i.p.). Cardiac function was evaluated at 3-, 6-, 12- and 18-hr after neuronostatin treatment in the first group of animals. For Western blot analysis, a second cohort of mice were sacrificed under anesthesia (ketamine 80 mg/kg and xylazine 12 mg/kg, i.p.) at 6-hr after neuronostatin injection.

Echocardiographic assessment

Three, six, twelve and eighteen hrs following neuronostatin (50 μg/kg, i.p.) treatment cardiac geometry and function were evaluated in anesthetized (ketamine 80 mg/kg and xylazine 12 mg/kg, i.p.) mice using

a 2-dimensional (2-D) guided M-mode echocardiography (Sonos 5500,Phillips Medical System, Andover, MA, USA) with a 15–6 MHz linear transducer. Pre-treatment measures were taken as controls. Fractional shortening was calculated from left ventricular (LV) end-diastolic diameter (LVEDD) and LV end-systolic diameter (LVESD) using the following equation: (LVEDD – LVESD)/LVEDD [13].

Isolation of murine cardiomyocytes

Murine cardiomyocytes were enzymatically isolated as described [13]. Briefly, under anesthesia (ketamine 80 mg/kg and xylazine 12 mg/kg, i.p.), hearts were removed and perfused with oxygenated (5% CO_2/95%O_2) Krebs-Henseleit bicarbonate (KHB) buffer consisting of 118 mM NaCl, 4.7 mM KCl, 1.2 mM $MgSO_4$, 1.2 mM KH_2PO_4, 25 mM $NaHCO_3$, 10 mM 4-(2-hydroxyethyl)-1-piperazineethanesulfonic acid (HEPES) and 10 mM glucose, at pH 7.35. The heart was then digested with a Ca^{2+}-free KHB buffer containing liberase blendzyme 4 (Hoffmann-La Roche Inc., Indianapolis, IN, USA) for 20 min. Left ventricles were removed and minced to disperse cardiomyocytes in Ca^{2+}-free KHB buffer after digestion. Extracellular Ca^{2+} was added incrementally back to 1.25 mM over a period of 30 min. Only rod-shaped cardiomyocytes with clear edges were selected for mechanical and intracellular Ca^{2+} studies within 8 hrs of isolation.

Cell shortening and relengthening

Mechanical properties of cardiomyocytes were measured using a SoftEdge MyoCam® system (IonOptix Corporation, Milton, MA). In brief, cardiomyocytes were placed in a chamber mounted onto the stage of an Olympus IX-70 inverted microscope and perfused with a contractile buffer containing: 131 mM NaCl, 4 mM KCl, 1 mM CaCl2, 1 mM MgCl2, 10 mM glucose and 10 mM HEPES, at pH 7.4. Cells were field-stimulated with a supra-threshold voltage at a frequency of 0.5 Hz, 3 msec in duration using a pair of platinum wires placed on opposite sides of the chamber connected to an electrical stimulator (FHC stimulator, Brunswick, NE, USA). The cardiomyocytes being studied were displayed on the computer monitor using an IonOptix MyoCam camera and cell length was captured during shortening and relengthening. Cell shortening and relengthening were evaluated using the following indices: peak shortening (PS, indicating peak ventricular contractility), maximal velocity of shortening (+ dL/dt), maximal velocity of relengthening (-dL/dt), time-to-PS (TPS, indicating contraction duration), time-to-90% relengthening (TR_{90}, indicating relaxation duration) [14].

Intracellular Ca2+ fluorescence measurement

Cardiomyocytes were loaded with fura-2/AM (0.5 μM) for 10 min and fluorescence measurements were recorded with a dual-excitation fluorescence photo multiplier system (Ionoptix). Cardiomyocytes were placed on an Olympus IX-70 inverted microscope and observed using Fluor ×40 oil objective. Cells were stimulated at 0.5 Hz and excited at 360 and 380 nm, with fluorescence emissions were detected between 480 and 520 nm by a photomultiplier tube after first illuminating the cells at 360 nm for 0.5 s, then at 380 nm for the duration of the recording. The 360 nm excitation scan was repeated at the end of the protocol, and qualitative changes in intracellular Ca^{2+} concentration were inferred from the ratio of fura-2 fluorescence intensity (FFI) at two wavelengths (360/380). Fluorescence decay time was assessed as an indication of the intracellular Ca^{2+} clearing rate. Intracellular Ca^{2+} transient decay constant was calculated using single and bi-exponential curve fit [15].

Western blotting

Myocardial proteins were prepared as previously described [15]. Briefly, heart tissues were homogenized using a RIPA lysis buffer, sonicated, and centrifuged at 12,000 xg for 20 min at 4°C. Tris-buffered saline/Tween 20 and protein concentrations of supernatants were measured using the Bradford assay. Samples were separated on a 7%, 10%, 12%,or 15% SDS-PAGE gel in a mini-gel apparatus (Mini-PROTEAN II, Bio-Rad, Hercules, CA, USA) and were then transferred to nitrocellulose membranes (0.2 mm pore size, Bio-Rad). Membranes were blocked for 1 hr in 5% nonfat milk in TBS-Tween and were incubated overnight at 4°C with anti-phospho-Akt (1:1,000), anti-Akt (1:1,000), anti-phospho-AMPK (1:1,000), anti-AMPK (1:1,000), anti--phospho-ERK1/2 (1:1,000), anti-ERK1/2 (1:1,000), anti-phospho-p38MAPK (1:1,000), anti-p38 MAPK (1:1,000), anti-phospho-JNK (1:1,000), anti-JNK (1:1,000), anti-phospho-CaMKII (1:1,000), anti-CaMK II (1:1,000), anti-phospho-Troponin I (1:1,000), anti-Troponin I (1:1,000), anti-phospho-Phospholamban pPLB,1:1,000), anti-pPhospholamban (PLB,1:1,000), anti-phospho-SERCA2α

Table 1. Biometric parameters in mice challenged with or without neuronostatin (50 μg/kg, i.p.). Mean ± SEM, n = 8 mice per group, p > 0.05 between groups for all indices evaluated

Parameter	Control	Neuronostatin
Body weight (g)	26.6 ± 0.8	28.4 ± 0.2
Heart weight (mg)	123 ± 5	130 ± 7
Heart weight/body weight (mg/g)	4.62 ± 0.21	4.58 ± 0.24
Liver weight (g)	1.46 ± 0.03	1.45 ± 0.05
Liver weight/body weight (mg/g)	55.1 ± 1.9	51.0 ± 1.7
Kidney weight (mg)	328 ± 9	348 ± 9
Kidney weight/body weight (mg/g)	12.3 ± 0.3	12.3 ± 0.4
Spleen weight (mg)	62.5 ± 4.8	75.0± 6.5
Spleen weight/body weight (mg/g)	2.35 ± 0.17	2.64 ± 0.22

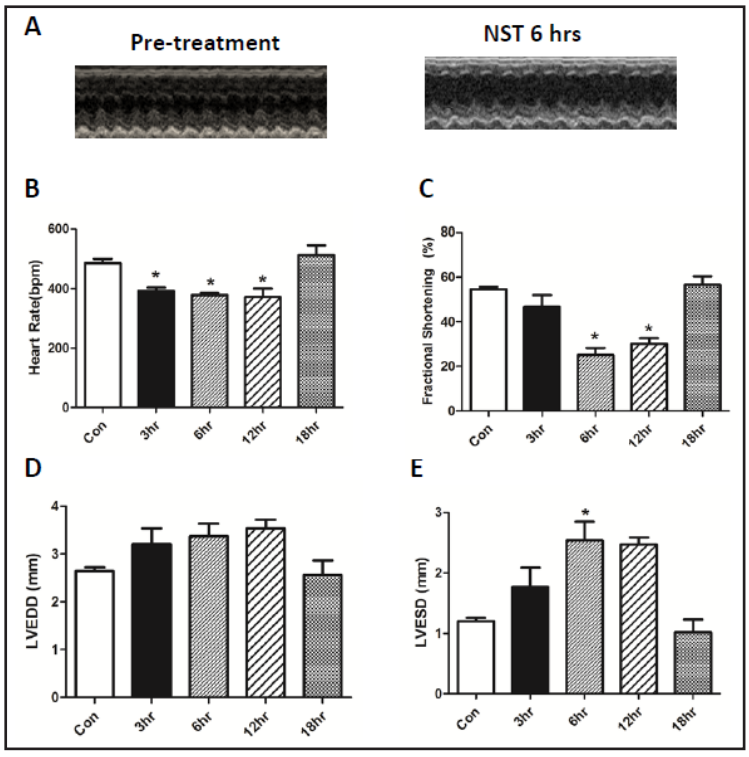

Fig. 1. Echocardiographic properties in C57 BL/6 mice treated with or without neuronostatin (NST, 50 μg/kg, i.p.) for 3, 6 and 18 hrs. A: Representative echocardiographic image from C57 BL/6 mice treated with or without neuronostatin; B: Heart rate; C: Fractional shortening (%); D: LV end diastolic diameter (LVEDD); and E: LV end systolic(LVESD), * p < 0.05 *vs.* control group.

(1:1,000), anti-SERCA2α (1:1,000), anti-GADPH (1:1,000) and anti-α-Tubulin (1:1,000). Antibodies were all purchased from Cell Signaling Technology (Beverly, MA) and Santa Cruz Biotechnology (Santa Cruz, CA). Membranes were then incubated for 60 min with HRP-conjugated secondary antibody (1:5,000) and detected by enzymatic chemiluminescence by a Bio-Rad Calibrated Densitometer.

Statistical analysis

Data were presented as Mean ± SEM. Statistical comparison was estimated using the student's t-tests or one-way analysis of variation (ANOVA) followed by a Tukey's test for *post hoc* analysis. All statistics was performed using a GraphPad Prism 4.0 software (GraphPad, San Diego, CA). A p value less than 0.05 was considered statistically significant.

Results

General and echocardiographic properties in mice with or without neuronostatin challenge

Neuronostatin treatment did not affect body and organ weights (heart, liver, kidney and spleen) or size (normalized to body weight) in C57BL/6 mice (Table 1). Echocardiographic measurement revealed a remarkable drop in heart rate after 3-, 6- and 12-hr of neuronostatin challenge. In addition, neuronostatin treatment significantly decreased LVESD and fractional shortening without affecting LVEDD between 6 and 12 hrs following neuronostatin challenge, the effect of which returned to basal level 18-hr after neuronostatin treatment (Fig. 1).

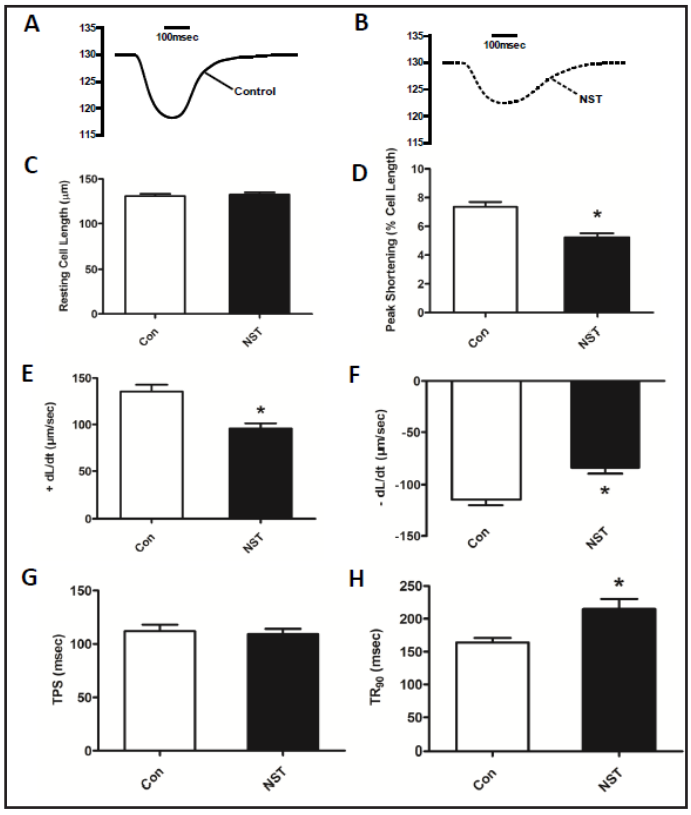

Fig. 2. Cardiomyocyte contractile properties in C57 BL/6 mice treated with or without neuronostatin (NST, 50 μg/kg, i.p.) for 6 hrs. A: Representative cell shortening trace of a cardiomyocyte from a C57 BL/6 control mouse; B: Representative cell shortening trace of a cardiomyocyte from a NST-treated mouse; C: Resting cell length; D: Peak shortening (normalized to cell length); E: Maximal velocity of shortening (+ dL/dt); F: Maximal velocity of relengthening (- dL/dt); G: Time-to-peak shortening (TPS); and H: Time-to-90% relengthening (TR_{90}). Mean± SEM, n= 90-105 cells from 3 mice per group, * $p < 0.05$ *vs.* control group.

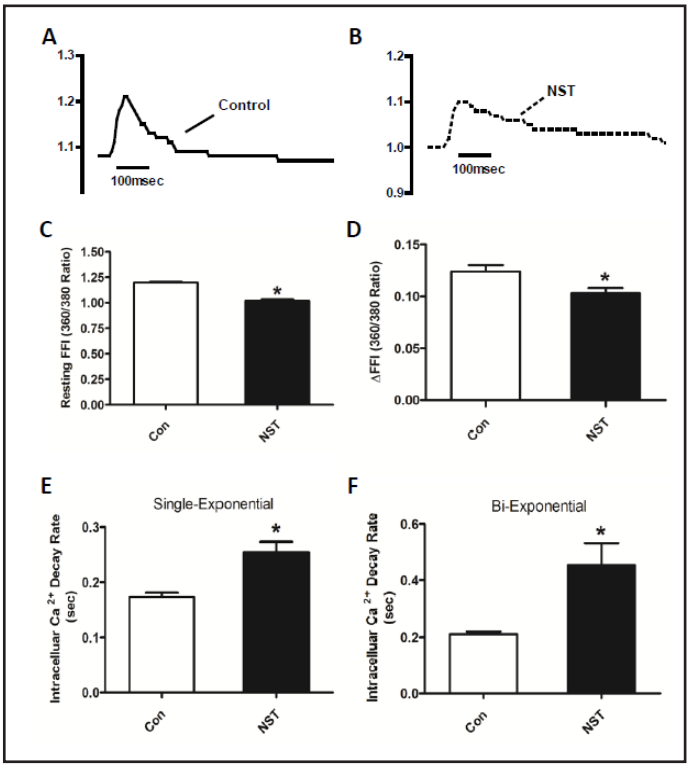

Fig. 3. Cardiomyocyte intracellular Ca^{2+} properties in C57 BL/6 mice treated with or without neuronostatin (NST, 50 μg/kg, i.p.) for 6 hrs. A: Representative intracellular Ca^{2+} Fura-2 fluorescence trace of a cardiomyocyte from a C57 BL/6 control mouse; B: Representative intracellular Ca^{2+} Fura-2 fluorescence trace of a cardiomyocyte from a NST-treated mouse; C: Resting fura-2 fluorescence intensity (FFI); D. Electrically-stimulated rise in FFI (ΔFFI); E: Intracellular Ca^{2+} transient decay rate (single-exponential); and F. Intracellular Ca^{2+} transient decay rate (bi-exponential). Mean ± SEM, n = 70–85 cells from 3 mice per group, * $p < 0.05$ *vs.* control group.

Effect of neuronostatin on cardiomyocyte contractile response

Neuronostatin exposure for 6-hr *in vivo* significantly depressed peaking shortening, reduced ± dL/dt, as well as prolonged TR_{90} without affecting TPS in murine cardiomyocytes. Resting cell length was unaffected by neuronostatin treatment (Fig. 2).

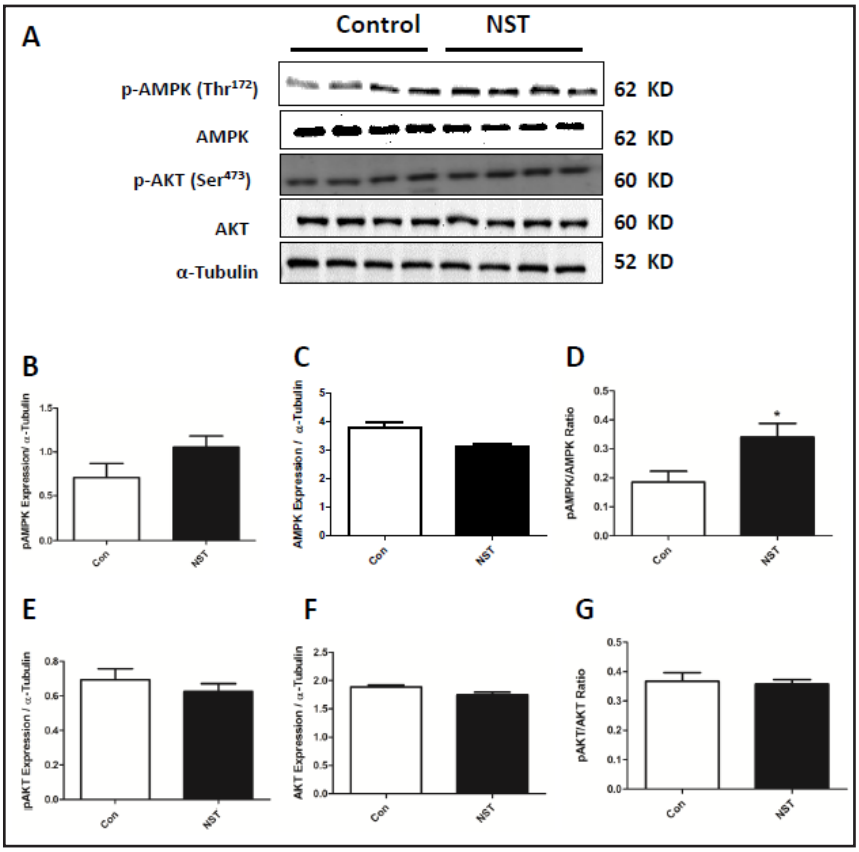

Fig. 4. Effect of neuronostatin-induced phosphorylation of AMPK and Akt. A: Representative gel blots depicting expression of pan and phosphorylated AMPK and Akt (α-tubulin used as loading control) using specific antibodies; B: Phospho-AMPK; C: AMPK; D: Phospho-AMPK-to-AMPK ratio; E: Phospho-Akt; F: Akt; and G: Phospho-Akt-to-Akt ratio; Mean± SEM, n = 4 per group, * $p < 0.05$ *vs.* control group.

Effect of neuronostatin on intracellular Ca^{2+} properties

To explore the possible mechanism behind neuronostatin-elicited mechanical changes, intracellular Ca^{2+} handling was measured using the Fura-2 fluorescence in cardiomyocytes from C57BL/6 mice with or without neuronostatin administration. Our data revealed that neuronostatin significantly decreased resting and electrically stimulated rise in intracellular Ca^{2+} (ΔFFI), as well as prolonged intracellular Ca^{2+} clearance (single or bi-exponential) (Fig. 3).

Effects of neuronostatin on activation of AMPK and Akt

To further elucidate the signaling mechanism involved in neuronostatin-induced cardiac response, the essential energy fuel signal AMPK and the cell survival mediator Akt were examined in murine hearts following neuronostatin challenge. Results in Fig. 4 depicted that neuronostatin significantly upregulated phosphorylation of AMPK (Thr^{172}) without affecting Akt (Ser^{473}) phosphorylation. Pan protein expression of AMPK and Akt was not affected by neuronostatin treatment.

Effects of neuronostatin on stress signaling ERK1/2, p38 MAP kinase and JNK

To explore if stress signal pathways contribute to neuronostatin-elicited cardiac responses, pan and phosphorylation of ERK1/2 (Thr^{202}/Tyr^{204}), p38 MAPK (Thr^{180}/Tyr^{182}) and JNK (Thr^{183}/Tyr^{185}) were examined in murine hearts following neuronostatin challenge. Our data shown in Fig. 5 do not favor a major role for stress signaling including p38 MAPK, JNK and ERK in neuronostatin-elicited cardiomyocyte response. Pan protein expression of ERK, MAPK and JNK was not affected by neuronostatin treatment.

Effect of neuronostatin on intracellular Ca^{2+} regulatory proteins

To explore the possible mechanism behind neuronostatin-induced myocardial responses, the intracellular Ca^{2+} regulatory proteins including SERCA2a, phospholamban and troponin

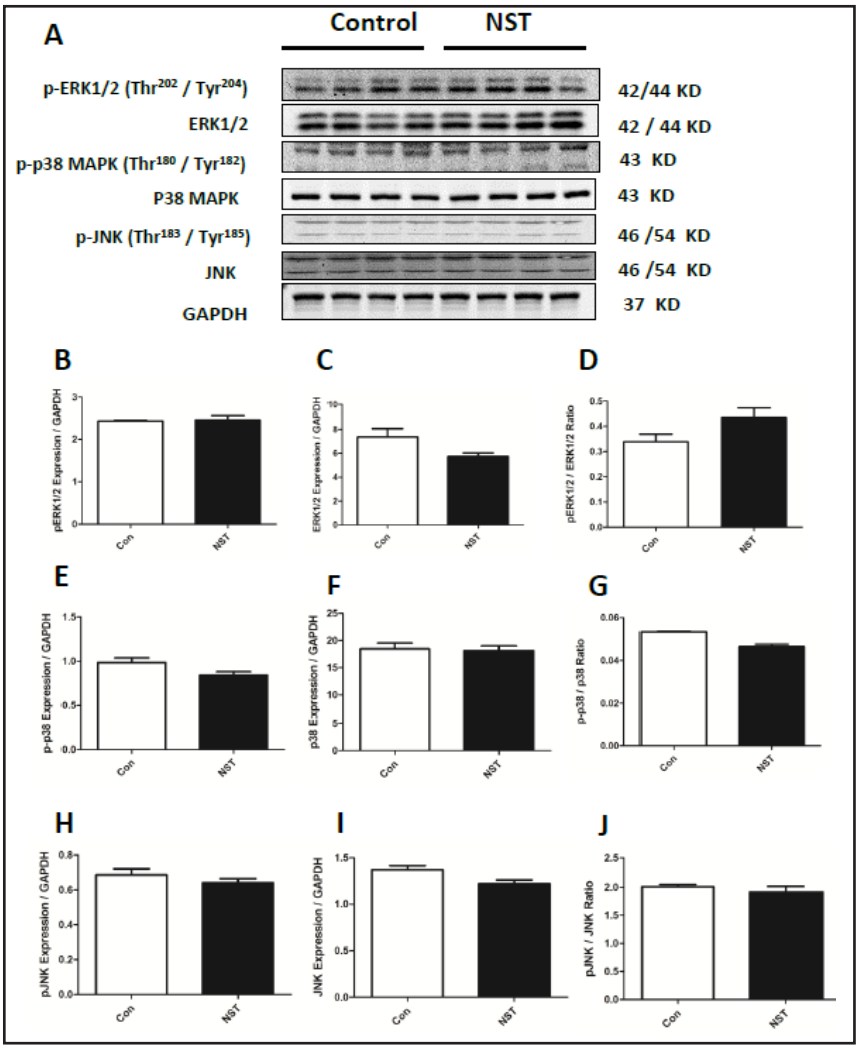

Fig. 5. Effect of neuronostatin-induced phosphorylation of ERK1/2, p38 MAPK and JNK. A: Representative gel blots depicting expression of pan and phosphorylated forms of ERK1/2, p38 MAPK, JNK and GADPH (loading control); B: Phospho-ERK1/2; C: ERK1/2; D: Phospho-ERK1/2-to-ERK1/2 ratio; E: Phospho-p38 MAPK; F: p38 MAPK; G: Phospho-p38 MAPK-to-p38 MAPK ratio; H: Phospho-JNK; I: JNK; and J: Phospho-JNK-to-JNK ratio. Mean ± SEM, n = 4 per group, * $p < 0.05$ *vs.* control group.

I were evaluated. Our results reveal that neuronostatin overtly downregulated total and phosphorylation of SERCA2a (Ser^{38}) without affecting expression or phosphorylation of PLB, an endogenous inhibitor of SERCA2a, following neuronostatin exposure *in vivo*. Meanwhile, enhanced phosphorylation of troponin I ($Ser^{23/24}$) was noted upon neuronostatin treatment, indicating a loss in myofilament Ca^{2+} sensitivity. There was little effect in the expression and activation of CaMK II (Thr^{286}) (Fig. 6).

Effect of AMPK and NOS inhibition on neuronostatin-induced cardiomyocyte responses

To examine the potential involvement of AMPK and NOS in neuronostatin-elicited cardiac response, isolated murine cardiomyocytes were pretreated with the AMPK inhibitor compound C (10 mM) [14] or the NOS inhibitor Nϖ-nitro-l-arginine methyl ester (L-NAME, 100 μM) [16] for 30 min prior to neuronostatin challenge (0.3 nM) [8]. Our results showed that compound C and L-NAME both abolished neuronostatin-induced inhibitory effects on PS, ± dL/dt and TR_{90} while eliciting little effect on cardiomyocyte mechanics themselves. These data favored a role of AMPK and NOS in neuronostatin-induced cardiac responses (Fig. 7).

Discussion

Neuronostatin was originally identified as a novel peptide encoded by the somatostatin gene. The salient findings from our current study revealed that the newly identified peptide

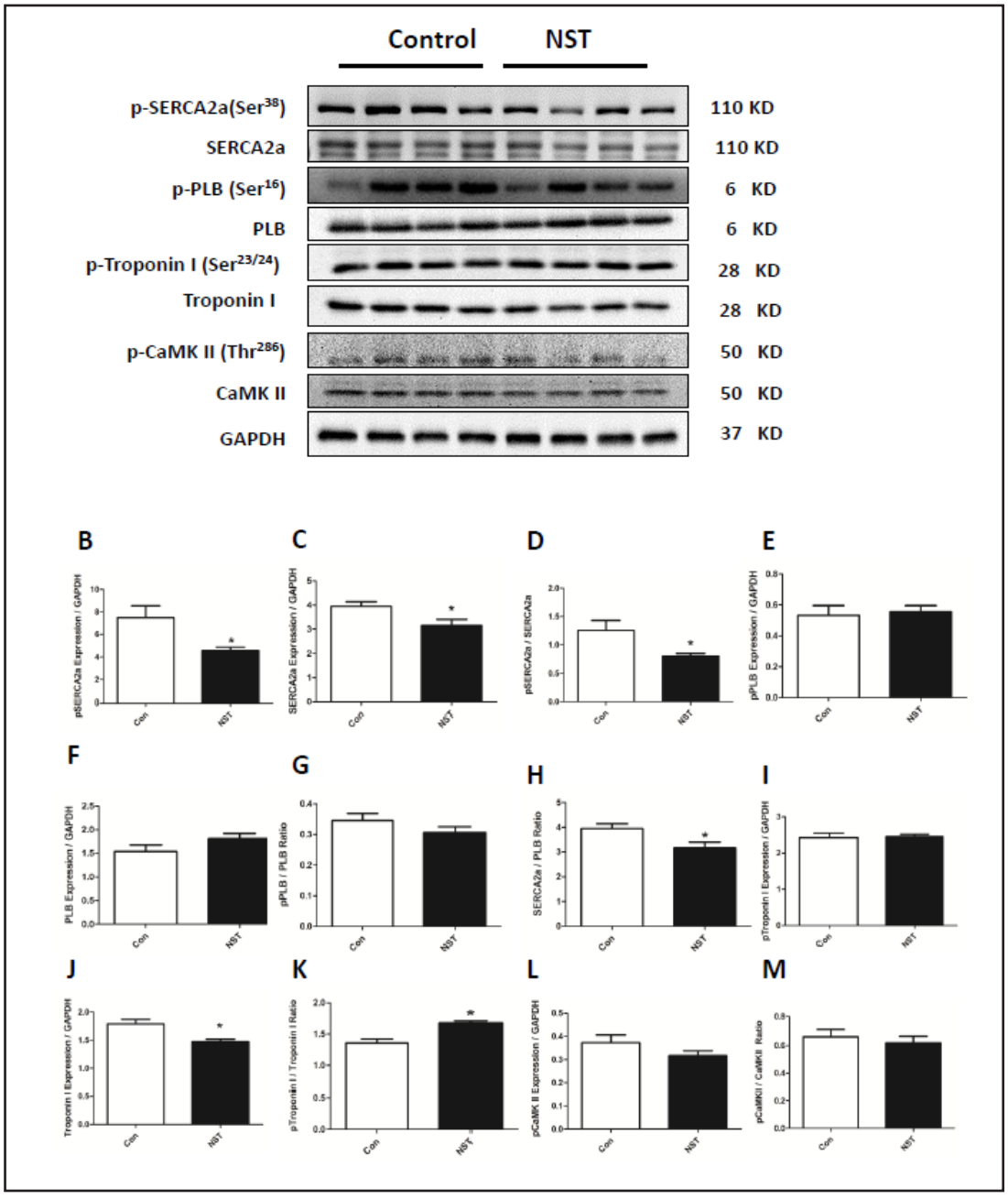

Fig. 6. Effect of neuronostatin-induced changes in intracellular Ca^{2+} regulatory proteins. A: Representative gel bots depicting expression of phospho-SERCA2a, SERCA2a, phospho- phospholamban(PLB, 5 kDa) , phospholamban (5 kDa), phospho-troponin I, troponin I, phospho-CaMK II, CaMK II and GAPDH (loading control); B. phospho-SERCA2a;C. pan SERCA2a; D Phospho-SERCA2a-to- SERCA2a ratio; E. phospho-PLB; F.pan PLB; G. Phospho-PLB-to-PLB ratio; H.SERCA2a/ PLB; I.phospho-Troponin; J pan Troponin I;K. Phospho-Troponin I-to-Troponin I ratio; L .phospho-CaMK II;M. Phospho-CaMK II-to- CaMK II ratio.

hormone neuronostatin is capable of eliciting cardiac remodeling, suppressing myocardial contractile function and intracellular Ca^{2+} handling including elevated LVESD, suppressed fractional shortening, peak shortening, maximal velocity of shortening/relengthening, resting and electrically-stimulated rise in intracellular Ca^{2+}, as well as prolonged duration of relengthening. These findings support the previous report that neuronostatin produces

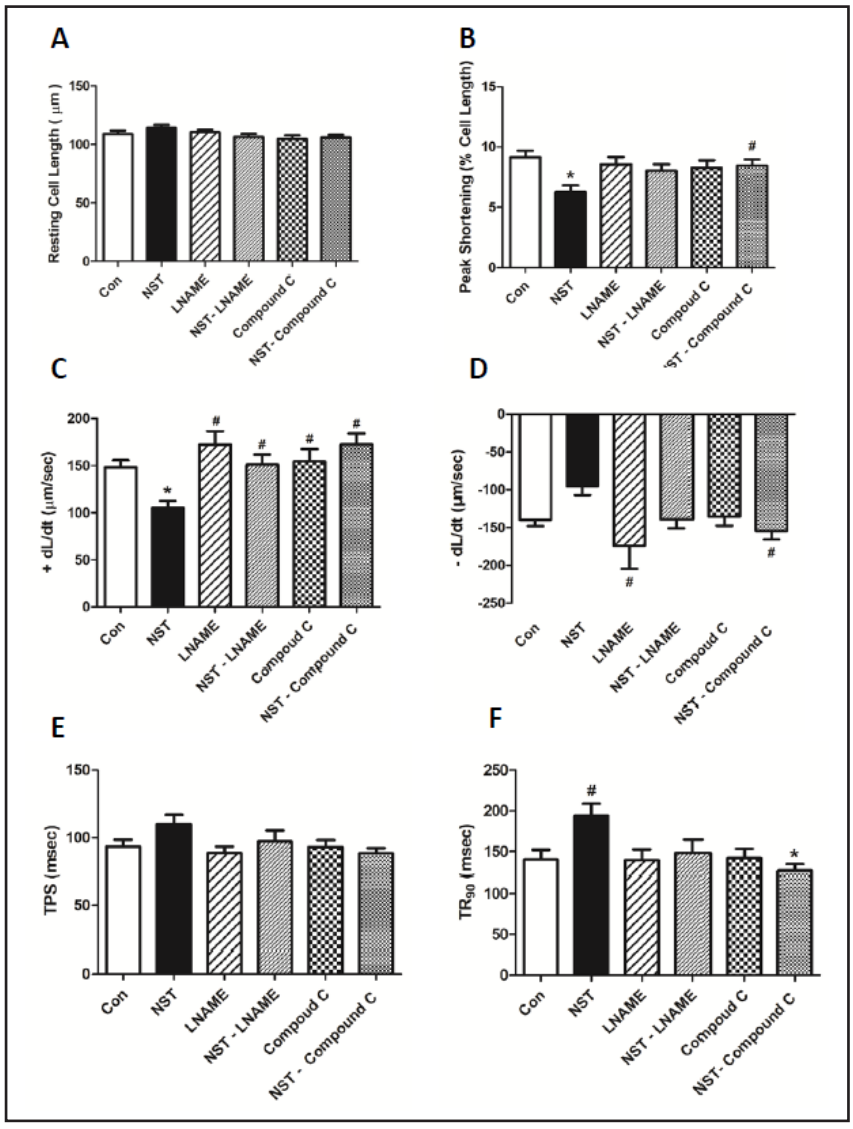

Fig. 7. Effects of the AMPK inhibitor Compound C (10 μM) and nitric oxide synthase (NOS) inhibitor Nϖ-nitro-l-arginine methyl ester (L-NAME,100 μM) on neuronostatin (0.3 nM)-induced cardiomyocyte contractile response.A: resting cell length; B: peak shortening (% of resting cell length); C: maximal velocity of shortening (+ dL/dt); D: maximal velocity of relengthening (– dL/dt); E: time-to-peak shortening (TPS); and F: time-to-90% re-lengthening (TR_{90}). Mean ± SEM, n = 54–56 cells per group, *p < 0.05 vs. control group; #p < 0.05 vs. NST group.

overt cardiac depressant action *in vitro* [8]. Moreover, our present findings revealed that neuronostatin-elicited cardiac depression may be mediated, at least in part, through AMPK as inhibition of AMPK using compound C effectively ablated neuronostatin-induced cardiac response. Meanwhile, the inhibitory effect of neuronostatin was causally associated with decreased SERCA2a and SERCA2a-to-phospholamban ratio, as well as phosphorylation of the SERCA inhibitory protein phospholamban (favoring a better SERCA activity). A greater phosphorylation of troponin I was also involved in the neuronostatin-mediated cardiac depression and intracellular Ca^{2+} mishandling. Our results did not favor any involvement of ERK1/2, p38 MAPK and JNK in neuronostatin-induced cardiac dysfunction. These observations suggest that endogenous neuronostatin, originating in cardiac afferents, may exert negative regulatory action on myocardial contractile function.

Observation from our study revealed impaired intracellular Ca^{2+} handling in particular decreased ΔFFI and prolonged intracellular Ca^{2+} decay following neuronostatin treatment, which may be attributed to defective contractile and intracellular Ca^{2+} transport/regulatory proteins [17], reduced intracellular Ca^{2+} availability resulted from poor SR Ca^{2+} load [18], and altered myofilament Ca^{2+} sensitivity [19]. Ample evidence has depicted that defects in SR Ca^{2+} handling are related with attenuated contractility [17, 18, 20]. SERCA2a is a cellular component governing regulation of SR Ca^{2+} cycling (including cytosolic Ca^{2+} removal and SR Ca^{2+} load), en route to fine maintenance of myocardial contraction and relaxation [18, 20].

Phospholamban serves as an endogenous inhibitor of SERCA2 to compromise the SERCA2a affinity for Ca^{2+} [10, 17, 21]. Our data revealed down-regulated total and phosphorylation of SERCA2a in conjunction with unchanged phospholamban pan protein expression and phosphorylation following neuronostatin exposure. The reduced SERCA2a level and SERCA2a/PLB ratio may account for, at least in part, intracellular Ca^{2+} mishandling and impaired relaxation (prolongation in relengthening duration and intracellular Ca^{2+} clearing). Cardiac troponin I (cTnI) is the key inhibitory element of the troponin complex, which regulates Ca^{2+} sensitivity and myocardial contraction [22]. Enhanced phosphorylation of troponin I following neuronostatin challenge suggests a loss in myofilament Ca^{2+} sensitivity in response to neuronostatin challenge. Troponin I ($Ser^{23/24}$) is phosphorylated by associated with PKA-dependent phosphorylation, which decreases myofilament Ca^{2+} sensitivity by reducing the Ca^{2+} binding affinity for TnC [23]. Ca^{2+} /Calmodulin-dependent protein kinase II (CaMKII) is considered another master regulator for intracellular Ca^{2+} cycling through its phosphorylation of phospholamban and RYR [24]. However, data from our current study did not favor a major role for CaMK II in neuronostatin exposure-induced cardiac response.

Our finding revealed that AMPK inhibition using compound C effectively negated neuronostatin-induced cardiac depressant responses, suggesting a role for AMPK in neuronostatin-induced cardiac action. AMPK, as a key energy sensor, is activated under conditions that deplete cellular ATP and elevate AMP levels response to energy deprivation in the heart, such as in heart failure [25]. AMPK may also be activated by hormones such as leptin and ghrelin [26, 27]. More importantly, inhibition of AMPK by compound C has been reported to slightly potentiate somatotrophic response to growth hormone-releasing hormone (GHRH) [28]. In our hands, neuronostatin augmented AMPK phosphorylation along with unchanged Akt phosphorylation. We suggest that neuronostatin may interrupt energy and metabolic balance, leading to decreased ATP availability, enhanced AMP/ATP ratio to turn on AMPK in the heart.

Recent evidence has identified a role for MAPK including ERK1/2, p38 MAPK and JNK involved in harmful cellular responses such as oxidative stress, DNA damage, hyperosmosis, low osmolarity and infection [29, 30]. In the heart, ERK1/2, p38 MAPK and JNK serve as important regulators for cardiac hypertrophy, interstitial fibrosis and cell survival [31, 32]. Somatostatin, a growth hormone inhibitory peptide, has been shown to play a key role in regulation of cell proliferation through modulation of MAPKs and cell survival pathway [33]. Findings from our current study do not favor a major role of stress signaling cascades including p38 MAPK and JNK in neuronostatin-elicited cardiomyocyte response *in vivo*, with the exception of ERK1/2. Although the precise mechanism responsible for the enhanced ERK1/2 phosphorylation in response to neuronostatin is unknown at this time, it may be related to a compensatory response to neuronostatin-induce pharmacological stress in the heart.

In conclusion, our current study demonstrated that neuronostatin attenuates myocardial contractile function and intracellular Ca^{2+} mishandling. The neuronostatin-elicited cardiac depression may be mediated, at least in part, through AMPK activation, loss of SERCA2a levels and SERCA2a-to-phospholamban ratio. These findings revealed not only a potent inhibitory capacity for neuronostatin on cardiac function, but also new insights for signaling mechanisms involved in neuronostatin-induced cardiac contractile anomalies. At this point, the precise mechanism responsible for neuronostatin-induced cardiac pathophysiological changes still remains elusive. Further studies should focus on better elucidation of cellular processes governing neuronostatin-induced biological effects.

Acknowledgements

This work was supported in part by NIH (5P20 GM432103) and the National Natural Foundation of China (No.81001566 and No.31271220).

Reference

1 Low MJ: Clinical endocrinology and metabolism. The somatostatin neuroendocrine system: physiology and clinical relevance in gastrointestinal and pancreatic disorders. Best Pract Res Clin Endocrinol Metab 2004;18:607-622.
2 Bell D, Zhao Y, McMaster B, McHenry EM, Wang X, Kelso EJ, McDermott BJ: SRIF receptor subtype expression and involvement in positive and negative contractile effects of somatostatin-14 (SRIF-14) in ventricular cardiomyocytes. Cell Physiol Biochem 2008;22:653-664.
3 Osadchii OE, Pokrovskii VM: [Somatostatin as a regulator of cardiovascular system functions]. Usp Fiziol Nauk 1998;29:24-41.
4 Maison P, Tropeano AI, Macquin-Mavier I, Giustina A, Chanson P: Impact of somatostatin analogs on the heart in acromegaly: a metaanalysis. J Clin Endocrinol Metab 2007;92:1743-1747.
5 Barros IC, Masuda MO, Aprigliano OQ: Electrophysiological effects of somatostatin at the supraventricular level of isolated guinea pig hearts. Braz J Med Biol Res 1992;25:289-299.
6 Samson WK, Zhang JV, Avsian-Kretchmer O, Cui K, Yosten GL, Klein C, Lyu RM, Wang YX, Chen XQ, Yang J, Price CJ, Hoyda TD, Ferguson AV, Yuan XB, Chang JK, Hsueh AJ: Neuronostatin encoded by the somatostatin gene regulates neuronal, cardiovascular, and metabolic functions. J Biol Chem 2008;283:31949-31959.
7 Yosten GL, Pate AT, Samson WK: Neuronostatin acts in brain to biphasically increase mean arterial pressure through sympatho-activation followed by vasopressin secretion: the role of melanocortin receptors. Am J Physiol Regul Integr Comp Physiol 2011;300:R1194-1199.
8 Hua Y, Ma H, Samson WK, Ren J: Neuronostatin inhibits cardiac contractile function via a protein kinase A- and JNK-dependent mechanism in murine hearts. Am J Physiol Regul Integr Comp Physiol 2009;297:R682-689.
9 Vainio L, Perjes A, Ryti N, Magga J, Alakoski T, Serpi R, Kaikkonen L, Piuhola J, Szokodi I, Ruskoaho H, Kerkela R: Neuronostatin, a novel peptide encoded by somatostatin gene, regulates cardiac contractile function and cardiomyocyte survival. J Biol Chem 2012;287:4572-4580.
10 Rodriguez P, Kranias EG: Phospholamban: a key determinant of cardiac function and dysfunction. Arch Mal Coeur Vaiss 2005;98:1239-1243.
11 Inesi G, Prasad AM, Pilankatta R: The Ca2+ ATPase of cardiac sarcoplasmic reticulum: Physiological role and relevance to diseases. Biochem Biophys Res Commun 2008;369:182-187.
12 Zhao P, Turdi S, Dong F, Xiao X, Su G, Zhu X, Scott GI, Ren J: Cardiac-specific overexpression of insulin-like growth factor I (IGF-1) rescues lipopolysaccharide-induced cardiac dysfunction and activation of stress signaling in murine cardiomyocytes. Shock 2009;32:100-107.
13 Xu X, Pacheco BD, Leng L, Bucala R, Ren J: Macrophage migration inhibitory factor plays a permissive role in the maintenance of cardiac contractile function under starvation through regulation of autophagy. Cardiovasc Res 2013;99:412-421.
14 Guo R, Scott GI, Ren J: Involvement of AMPK in alcohol dehydrogenase accentuated myocardial dysfunction following acute ethanol challenge in mice. PLoS One 2010;5:e11268.
15 Kandadi MR, Hua Y, Ma H, Li Q, Kuo SR, Frankel AE, Ren J: Anthrax lethal toxin suppresses murine cardiomyocyte contractile function and intracellular Ca2+ handling via a NADPH oxidase-dependent mechanism. PLoS One 2010;5:e13335.
16 Ren J, Wen Y, Hintz KK: Influence of hypertension on cardiac contractile response of human erythrocyte-derived depressing factor in ventricular myocytes. J Hypertens 2003;21:1183-1190.
17 Hadri L, Hajjar RJ: Calcium cycling proteins and their association with heart failure. Clin Pharmacol Ther 2011;90:620-624.
18 Vafiadaki E, Papalouka V, Arvanitis DA, Kranias EG, Sanoudou D: The role of SERCA2a/PLN complex, Ca(2+) homeostasis, and anti-apoptotic proteins in determining cell fate. Pflugers Arch 2009;457:687-700.
19 van der Velden J, Merkus D, Klarenbeek BR, James AT, Boontje NM, Dekkers DH, Stienen GJ, Lamers JM, Duncker DJ: Alterations in myofilament function contribute to left ventricular dysfunction in pigs early after myocardial infarction. Circ Res 2004;95:e85-95.
20 Hobai IA, O'Rourke B: Decreased sarcoplasmic reticulum calcium content is responsible for defective excitation-contraction coupling in canine heart failure. Circulation 2001;103:1577-1584.
21 MacLennan DH, Kranias EG: Phospholamban: a crucial regulator of cardiac contractility. Nat Rev Mol Cell Biol 2003;4:566-577.

22 Kobayashi T, Solaro RJ: Calcium, thin filaments, and the integrative biology of cardiac contractility. Annu Rev Physiol 2005;67:39-67.
23 Metzger JM, Westfall MV: Covalent and noncovalent modification of thin filament action: the essential role of troponin in cardiac muscle regulation. Circ Res 2004;94:146-158.
24 Anderson ME, Brown JH, Bers DM: CaMKII in myocardial hypertrophy and heart failure. J Mol Cell Cardiol 2011;51:468-473.
25 Kim M, Tian R: Targeting AMPK for cardiac protection: opportunities and challenges. J Mol Cell Cardiol 2011;51:548-553.
26 Tulipano G, Giovannini M, Spinello M, Sibilia V, Giustina A, Cocchi D: AMP-activated protein kinase regulates normal rat somatotroph cell function and growth of rat pituitary adenomatous cells. Pituitary 2011;14:242-252.
27 Lim CT, Kola B, Korbonits M: AMPK as a mediator of hormonal signalling. J Mol Endocrinol 2010;44:87-97.
28 Shirwany NA, Zou MH: AMPK in cardiovascular health and disease. Acta Pharmacol Sin 2010;31:1075-1084.
29 Johnson GL, Lapadat R: Mitogen-activated protein kinase pathways mediated by ERK, JNK, and p38 protein kinases. Science 2002;298:1911-1912.
30 Pearson G, Robinson F, Beers Gibson T, Xu BE, Karandikar M, Berman K, Cobb MH: Mitogen-activated protein (MAP) kinase pathways: regulation and physiological functions. Endocr Rev 2001;22:153-183.
31 Wang Y: Mitogen-activated protein kinases in heart development and diseases. Circulation 2007;116:1413-1423.
32 Petrich BG, Wang Y: Stress-activated MAP kinases in cardiac remodeling and heart failure; new insights from transgenic studies. Trends Cardiovasc Med 2004;14:50-55.
33 Florio T, Thellung S, Arena S, Corsaro A, Bajetto A, Schettini G, Stork PJ: Somatostatin receptor 1 (SSTR1)-mediated inhibition of cell proliferation correlates with the activation of the MAP kinase cascade: role of the phosphotyrosine phosphatase SHP-2. J Physiol Paris 2000;94:239-250.